

Modification to the flow properties of repository cement as a result of carbonation

G. PURSER*, A. E. MILODOWSKI, D. J. NOY, C. A. ROCHELLE, J. F. HARRINGTON, A. BUTCHER & D. WAGNER

British Geological Survey, Environmental Science Centre, Keyworth, Nottingham NG12 5GG, UK

**Corresponding author (e-mail: gemm@bgs.ac.uk)*

Abstract: A UK repository concept currently under consideration for the disposal of intermediate-level radioactive waste and some low-level waste not suitable for surface disposal involves using large quantities of cementitious materials for construction, grouting, waste containers, waste isolation matrix and buffer/backfill. CO₂ generated from the degradation of organic material in the waste will result in cement carbonation and associated mineralogical changes. Hydraulic and gas permeability tests were performed on Nirex Reference Vault Backfill (NRVB) cement at 40 °C and either 4 or 8 MPa. Carbonation reactions using CO₂ gas halved the permeability of the NRVB under simulated repository conditions. A greater decrease in permeability (by three orders of magnitude) was found during carbonation using dissolved CO₂. Mineralogical changes were found to occur throughout the cement as a result of the reaction with CO₂. However, a narrow zone along the leading edge of a migrating reaction front was associated with the greatest decrease in porosity. Fluid pressures increased slightly due to permeability reductions but fluid flow still continued (albeit at a lower rate) preventing the build-up of overly high pressures. Overall, the observed reductions in permeability could be beneficial in that they may help reduce the potential for fluid flow and radionuclide migration. However, continued carbonation could lead to potential issues with regards to gas pressure build-up.

In the UK, a repository concept for the disposal of intermediate-level radioactive waste and some low-level waste involves using large quantities of cementitious materials for both construction, grout sealing, waste isolation matrix, waste containers and buffer/backfill (Crossland 1998). Some of the waste will generate gas (methane, CO₂ and hydrogen) and waste canisters will be fitted with ports to allow them to vent. Nirex Reference Vault Backfill (NRVB) cement (Francis *et al.* 1997), which might be used as a backfill material in a UK geological disposal facility (GDF), is specifically designed to have a relatively high permeability to allow some fluid flow to prevent the build-up of pressure in the repository, whilst retaining the capacity to buffer the pore water to an alkaline pH (>12.5) for a significant period following repository closure, in order to limit the mobility of many of the radionuclides.

Degradation of organic materials present in the wastes may produce significant quantities of carbon dioxide (CO₂). This will initiate carbonation reactions which will reduce the high pH buffering capacity of the cement due to the alteration of cement phases to secondary carbonate phases, such as calcite (Crossland 1998). This neutralization of alkaline conditions may have two impacts on the repository: first, there may be an increased

potential for steel corrosion; and, secondly, there is an increased likelihood of radionuclide mobilization under lower pH conditions. These carbonation reactions may also alter cement physical properties, and change porosity, permeability and, possibly, strength. The aim of this study was to determine the impacts of NRVB carbonation on fluid flow under simulated repository conditions.

In the current UK concept for a radioactive waste repository there would be a mined facility between 400 and 800 m below the surface (Crossland 1998). At 400 m, the likely *in situ* pore pressure would be 4 MPa, with a temperature of around 40 °C based on the geothermal gradient. CO₂ in this instance would be present in a gaseous form. However, at 800 m (pore pressure 8 MPa), CO₂ would exist as a dense, supercritical phase (Fig. 1). In this study, we conducted experiments that covered this potential range of *in situ* conditions simulating both gaseous and dissolved CO₂. However, we acknowledge that it is unlikely that CO₂ could be generated fast enough for supercritical CO₂ to exist in the repository but was included as an extreme case. In this paper, we summarize the results from four experiments where we compare flow property changes with mineralogical alteration, and also with coupled reaction–transport simulations.

From: SHAW, R. P. (ed.) *Gas Generation and Migration in Deep Geological Radioactive Waste Repositories*. Geological Society, London, Special Publications, **415**, <http://dx.doi.org/10.1144/SP415.9>

© 2014 The Author(s). Published by The Geological Society of London. All rights reserved. For permissions: <http://www.geolsoc.org.uk/permissions>. Publishing disclaimer: www.geolsoc.org.uk/pub_ethics

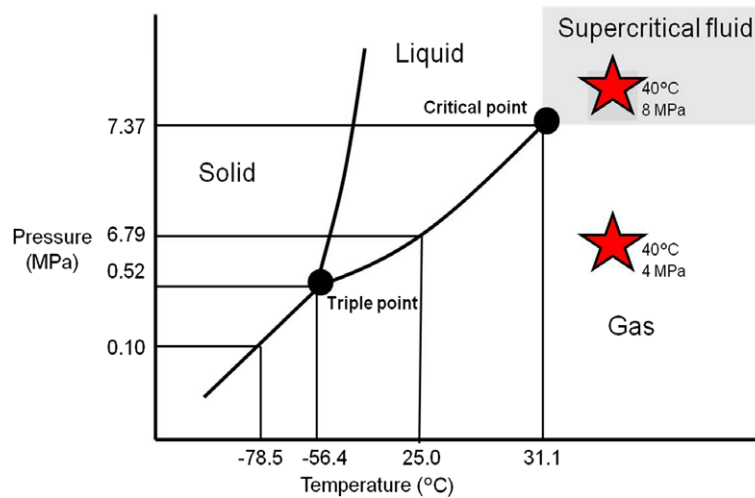


Fig. 1. Phase diagram for CO₂. The areas represented as stars (red in online version) in the diagram show the range of experimental conditions used during this study (modified after Atkins 1982).

Further details of the experiments are given in Purser *et al.* (2014).

Methods

NRVB preparation

NRVB has been used in previous experimental work on radioactive waste storage in the UK (Francis *et al.* 1997). It is acknowledged, however, that the compositions of backfill cements used in any future repository may well be different to the composition used in this study but it is considered that many of the mineralogical reactions we observed are likely to be common to a wide range of cements.

Samples of NRVB were prepared in one 29 kg batch using the following composition and added sequentially in the following order (Francis *et al.* 1997):

- (1) water (tap water) (10.15 kg);
- (2) Portland cement ('Ordinary Portland cement', from Hanson) (7.50 kg);
- (3) limestone flour ('Superlon 100', from Longcliffe Ltd) (8.25 kg);
- (4) lime ('Hydralime', from Lafarge) (2.83 kg).

The components were mixed using a portable cement mixer set at approximately 70 rpm for 30 min to produce fine uniform slurry that was poured into cylindrical moulds. These were allowed to set in an oven at 40 °C for 24 h. The cylinders of cement were then demoulded and cured in Ca(OH)₂-saturated water for a further 28 days at 40 °C. They were stored in Ca(OH)₂-saturated water at room temperature to prevent the cores drying out or being

carbonated by atmospheric CO₂. The cylinders of cement were subcored symmetrically down the central axis to produce samples, 49 mm in diameter × 49 mm long. The final dimensions were accurately measured using a Linear Tools electronic calliper and the sample weight was measured using a Mettler AT460 digital balance.

Experimental set-up

The core samples were placed between sintered stainless steel filters (to aid fluid distribution across the face of the sample) and stainless steel end caps. A Teflon jacket was used to exclude the confining fluid, deionized water. Volumetric flow rates into and out of the samples were controlled and monitored using a pair of ISCO-500HP, series D, syringe pumps operated from a single digital control unit, linked to remotely operated LabView™ software (Fig. 2). Data collection was performed every 2 min. A subsample of these data (a smoothed average of data points selected every 16 min) was used for the final data analysis. The injection fluid (gas or liquid) and sample assembly were housed inside a fan-assisted Binder oven set to 40 °C (±0.5 °C) to reduce the effect of thermal noise on the flow data.

Testing flow properties

A typical experiment comprised a series of test stages: initially the sample was resaturated, followed by hydraulic testing and then a gas-injection test. These stages were sometimes repeated more than once within any one experiment to identify

MODIFICATION IN CEMENT FLOW PROPERTIES

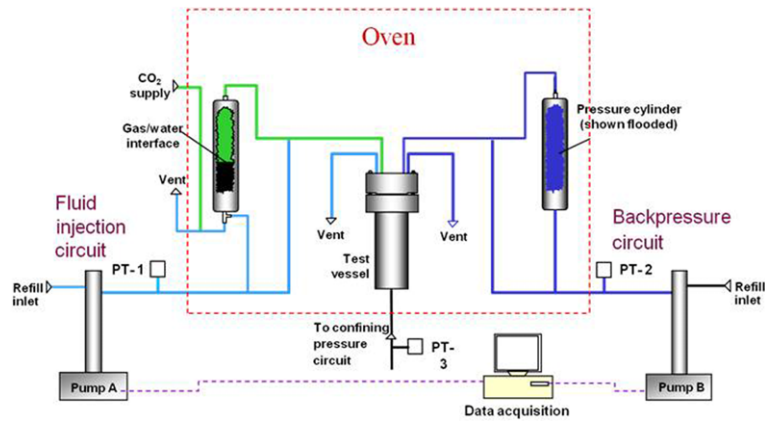


Fig. 2. Experimental instrumentation for hydraulic and gas testing.

any changes to the NRVB flow properties. Four samples of NRVB were successfully tested in this study, and the sequence of experimental test stages is detailed in Table 1.

Resaturation. Each core sample was resaturated using $\text{Ca}(\text{OH})_2$ -saturated water in the interface vessel to re-equilibrate the sample after sample preparation (or, in one case, to remove injected nitrogen (N_2)). Other studies (Francis *et al.* 1997) used deionized water for this purpose but this could have caused unwanted mineral dissolution, which, if extensive, could inadvertently lead to decreases in changing sample porosity and permeability.

Hydraulic tests. Hydraulic testing was performed in most cases using $\text{Ca}(\text{OH})_2$ -saturated water. The injection and backpressure pumps were maintained at either 4 or 8 MPa during initial core

saturation. Hydraulic testing commenced by increasing and then decreasing the injection flow rate in a stepwise manner, sequentially doubling or halving the flow rate (Fig. 3). Values used were 2125, 4250 and $8500 \mu\text{l h}^{-1}$. In one experiment, the water used for hydraulic testing was saturated with CO_2 at 4 MPa to allow the impact of dissolved CO_2 on hydraulic permeability and conductivity to be assessed.

Gas-injection tests. Two gas types were used: N_2 to provide baseline data (inert case) or CO_2 in either a gaseous (4 MPa) or supercritical state (8 MPa). These were accurately displaced from the injection interface vessel (Fig. 2) using deionized water and through the NRVB sample. The initial pressure in both the injection and backpressure lines was set to a constant 4 or 8 MPa. Once each test system had stabilized, gas was injected into

Table 1. Sequence of experimental test stages for the four NRVB cement cores tested

Stage	Test type	Experiment/core number			
		1	2	3	4
1	Resaturation	$\text{Ca}(\text{OH})_2$ -saturated water	$\text{Ca}(\text{OH})_2$ -saturated water	$\text{Ca}(\text{OH})_2$ -saturated water	$\text{Ca}(\text{OH})_2$ -saturated water
2	Hydraulic test	$\text{Ca}(\text{OH})_2$ -saturated water	$\text{Ca}(\text{OH})_2$ -saturated water	$\text{Ca}(\text{OH})_2$ -saturated water	$\text{Ca}(\text{OH})_2$ -saturated water
3	Gas test	–	Gaseous N_2	Supercritical CO_2	Gaseous CO_2
4	Resaturation	–	$\text{Ca}(\text{OH})_2$ -saturated water	–	–
5	Hydraulic test	CO_2 saturated water	$\text{Ca}(\text{OH})_2$ -saturated water	–	–
6	Gas test	–	Gaseous CO_2	–	–
7	Gas test	–	Gaseous N_2	–	–
Starting pressure (MPa)		4	4	8	4
Temperature ($^{\circ}\text{C}$)		40	40	40	40

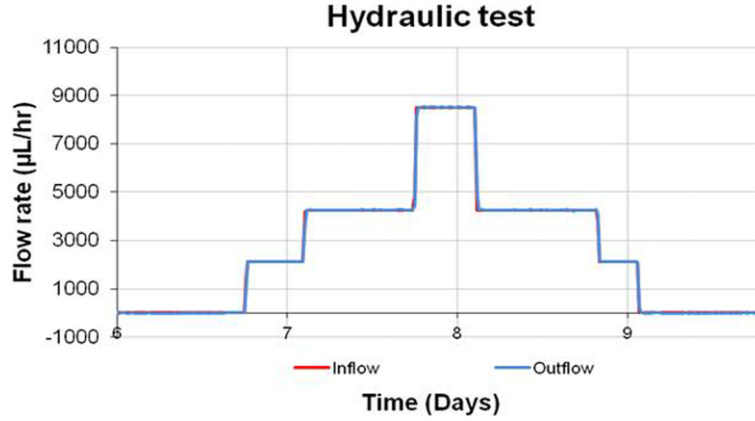


Fig. 3. Hydraulic test using $\text{Ca}(\text{OH})_2$ -saturated water showing a rapid transmission of fluid across the sample (inflow and outflow lines overlap on the chart), with the outflow being equivalent to the inflow at each test flow rate.

the NRVB sample at a constant flow rate (initially $1250 \mu\text{l h}^{-1}$).

Both hydraulic and gas permeability data were calculated using the following equations when the experiment had reached a steady state (Harrington & Horseman 1999).

Hydraulic permeability:

$$k = \frac{Q_w \eta_w L_s}{A_s (\rho_{wi} - \rho_{wo})}$$

where k is the intrinsic permeability of the porous medium (m^2), Q_w is the volumetric flux of water, η_w is the viscosity of water (Pa s), L_s is the length of the sample (mm), A_s is the cross-sectional area of the sample, ρ_{wi} is the pressure of the water inlet (Pa) and ρ_{wo} is the pressure of water outlet (Pa).

Gas permeability:

$$k_g = \frac{2Q_{st}RT\eta_g L_s}{v_{mst}A_s [p_{gi}^2 - (p_{wo} + p_{co})^2]}$$

where k_g is the intrinsic gas permeability of the porous medium (m^2), Q_{st} is the volumetric flux of gas under STP ($\text{m}^3 \text{s}^{-1}$), v_{mst} is the partial molar volume of gas under STP ($\text{m}^3 \text{mol}^{-1}$), R is the gas constant, T is temperature (K), p_{wo} is the backpressure of water (Pa), p_{co} is the matric suction, η_g is the viscosity of gas (Pa s), L_s is the length of the sample (mm), A_s is the cross-sectional area of the sample and p_{gi} is the injection pressure of the gas (Pa).

Mineralogical preparation

On removal of the sample from the reaction vessel, the moist reacted cement core was dried under

vacuum ($c. 1 \times 10^{-1}$ torr) at 18°C until a constant weight was reached. The dry cement core was sliced in half (parallel to the core axis), producing two half cores for analysis. An unreacted cement sample, which had been stored in water saturated with $\text{Ca}(\text{OH})_2$ for the duration of the experiments, was prepared in the same way and used as a comparison during mineralogical assessment of the impact of carbonation of NRVB.

Half core 1: The sample was vacuum impregnated with a blue-dyed epoxy resin to allow the porosity in the cement to be easily observed. A polished thin section cut parallel to the direction of flow was then produced for mineralogical analysis by optical transmitted light microscopy and backscattered electron microscopy with an energy-dispersive X-ray microanalysis system (BSEM-EDXA).

Half core 2: This sample was initially used for micropermeameter analysis. Micropermeameter measurements were made along the length of the cut flat face of the half core using a Temco MP-402 mini-permeameter. The face was prepared using adhesive peels to remove cutting fines from the surface. Measurements were repeated several times at the same point and the mean figure taken as the representative gas permeability. Gas permeability, k_a , was calculated from the following equation:

$$k_a = \frac{2\mu Q_b P_b T_{act}}{aG_0 (P_1^2 - P_2^2) T_{ref}}$$

where k_a is the gas permeability (mD), μ is viscosity (cP), Q_b is the volumetric flow rate ($\text{cm}^3 \text{s}^{-1}$), P_b is the reference pressure (atm), T_{act} is the actual temperature ($^\circ\text{C}$), T_{ref} is the reference temperature ($^\circ\text{C}$), G_0 is the dimensionless geometric shape factor, a

MODIFICATION IN CEMENT FLOW PROPERTIES

is the internal radius of the tip of the permeameter (cm), and P_1 and P_2 are the upstream and downstream pressure (atm), respectively.

The same sample was used to determine CO_2 content by dissolving approximately 27 g of sample using 4 M hydrochloric acid solution in a glass beaker. The volume of acid used for dissolution was 250 g for unreacted NRVB core and 530 g for the carbonated core sample from Experiment 2. CO_2 was given off as the carbonate minerals in the sample dissolved, and the weight of CO_2 in the sample was calculated from the overall weight of the beaker before and after dissolution.

Modelling. Preliminary modelling using PRECIP (Noy 1998), a single fluid-phase one-dimensional (1D) reaction-transport code, was used to model the mineral reactions occurring within the sample in the presence of dissolved CO_2 using the following parameters:

- core length: 49 mm;
- porosity: 52%;
- injection flow rate: $2000 \mu\text{l h}^{-1}$;
- fluid composition: water equilibrated with CO_2 at 4 MPa and calcite;
- master aqueous species: Ca^{2+} , HCO_3^- , H^+ and SiO_2 ;
- minerals: quartz, chalcedony, calcite, portlandite and tobermorite;
- aqueous products: CO_2 (aq), CO_3^{2-} , CaCO_3 , CaHCO_3^+ , HSiO_3^- , $\text{H}_2\text{SiO}_4^{2-}$, OH^- .

Two cases were explored:

- (1) A base case was run using the standard dissolution and precipitation rates for each mineral.

- (2) A second case was then run using reduced rates, by a factor of 2.5, for tobermorite dissolution, and chalcedony and aragonite precipitation. This was performed to determine how mineral reaction kinetics would affect the reaction zone in the simulated model and help to better understand the reaction processes.

Results

Hydraulic testing of all NRVB cement samples

Hydraulic testing was performed on all NRVB samples after resaturation. This repeat measurement on the four NRVB cores produced constant and highly reproducible bulk hydraulic permeability (Table 2). The overall average permeability of NRVB was found to be $4.3 \times 10^{-17} \pm 0.4 \times 10^{-17} \text{ m}^2$. It has been suggested that, for structural components of low-level radioactive waste disposal units, the hydraulic conductivity of the concrete should be less than 10^{-8} m s^{-1} to prevent water infiltration (Chau *et al.* 1995). Portland cement used in carbon capture and storage (CCS) applications may have an intrinsic permeability to gas as low as $14 \times 10^{-19} \text{ m}^2$ and to liquids $2 \times 10^{-19} \text{ m}^2$ (Fabbri *et al.* 2009). In comparison to these cement types and applications, NRVB has a relatively high permeability, consistent to its application as a backfill cement designed to be highly permeable to gas to aid dispersion and prevent any overly high-pressure build-ups in the repository. The reproducibility also indicated that the different samples gave comparable results, allowing subsequent gas tests to be compared with confidence.

Table 2. Calculated permeabilities of hydraulic and gas tests on the four NRVB core samples tested

Stage	Test type	Fluid	Permeability (m^2)				
			Experiment/core number				
			1	2	3	4	Average
1	Resaturation	Ca(OH)_2 fluid	–	–	–	–	–
2	Hydraulic test	Hydraulic test	4.3×10^{-17}	4.1×10^{-17}	4.0×10^{-17}	4.7×10^{-17}	4.3×10^{-17}
3	Gas test	N_2	–	2.0×10^{-19}	–	–	–
		Supercritical CO_2	–	–	2.0×10^{-19}	–	–
4	Resaturation	Ca(OH)_2 fluid	–	–	–	–	–
5	Hydraulic test	Ca(OH)_2 fluid	–	4.2×10^{-17}	–	–	–
		CO_2 saturated fluid	4.3×10^{-20}	–	–	–	–
6	Gas test	CO_2	–	9.9×10^{-20}	–	–	–
7	Gas test	N_2	–	1.1×10^{-19}	–	–	–

*Partial test only, no CO_2 permeability data.

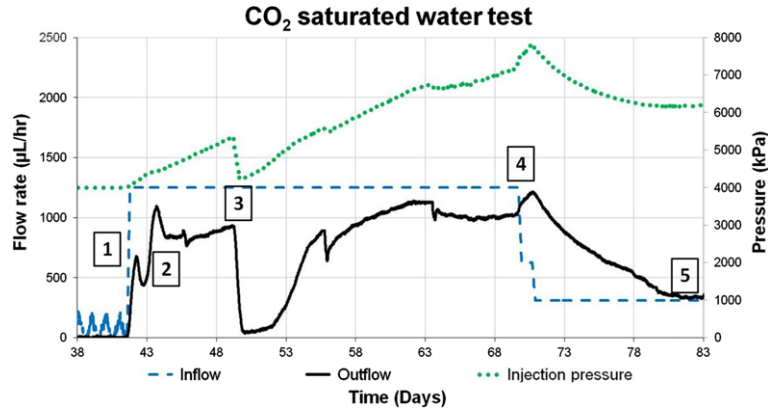


Fig. 4. Hydraulic test using CO₂-saturated fluid showing the stepped reduction in flow rate required to achieve steady state with this type of fluid. Numbers within squares represent specific events during the experiment.

Hydraulic testing: the effects of dissolved CO₂ (Experiment 1)

Prior to this test we realized that the addition of CO₂ to the Ca(OH)₂-saturated water would cause extensive precipitation of CaCO₃. Therefore we pre-equilibrated our standard Ca(OH)₂-saturated water with CO₂ at 40 °C and 4 MPa in a separate vessel. The fluid was then filtered and transferred at pressure into the injection interface vessel. The hydraulic test then commenced at an initial flow rate of 1250 µl h⁻¹ (Fig. 4). During the initial increase in the test flow rate (marked 1 in Fig. 4), the outflow from the sample did not rapidly match the inflow (marked 2 in Fig. 4). This was different to previous hydraulic tests conducted with the Ca(OH)₂-saturated water containing no CO₂ (Fig. 3). This suggests that the reaction of the CO₂ rapidly changed the flow within the sample.

On day 49 of the test, outflow decreased significantly (marked 3 on Fig. 4). This was attributed to an accidental change in the fluid type moving through the sample (from CO₂-saturated water to CO₂ gas). Although the temporary change from CO₂-saturated water to a 'slug' of CO₂ gas was unintended, it did demonstrate that CO₂ gas was able to pass through the carbonated cement very easily. The test continued using CO₂-saturated water at a flow rate of 1250 µl h⁻¹, and an increase in pressure to close to the 8 MPa confining pressure necessitated the flow rate being decreased to 625 µl h⁻¹ (marked 4 in Fig. 4) and finally 325 µl h⁻¹ before steady state was achieved (marked 5 in Fig. 4). CO₂-saturated water was found to decrease permeability by three orders of magnitude in comparison to standard hydraulic tests, and the permeability was determined to be 4.3 × 10⁻²⁰ m² (Table 2). Carbonation caused a reduction in permeability below

that of the cements used for CCS highlighted earlier. The permeability of the carbonated cement to gas such as CO₂ or N₂ was not tested in this instance.

Gas testing: flow properties of an inert gas (N₂) (Experiment 2)

N₂ was used to assess the movement of an inert gas through the NRVB. This produced a baseline case with which to compare the impact of CO₂ gas on transport properties. N₂ testing resulted in a calculated gas permeability of 2.0 × 10⁻¹⁹ m² (Table 2). A repeat hydraulic test with Ca(OH)₂-saturated water was performed after the N₂ gas test (Table 2, Stage 5, Test 2). As these data were comparable to the initial hydraulic data (Table 2, Stage 2, Test 2), it confirmed that testing with N₂ had no physical or chemical impact upon the NRVB. N₂ was also used to confirm changes in NRVB permeability due to cement carbonation following CO₂ gas testing (Table 2, Stage 7, Test 2).

Gas testing: flow properties of CO₂ gas (Experiment 2)

A test using gaseous CO₂ was performed at 40 °C and 4 MPa. In comparison to the N₂ base case, the gas breakthrough was relatively slow, taking 6 days rather than 2 days. We consider this a consequence of the carbonation reactions consuming much of the ingressing CO₂. These reactions may have been the cause of a build-up of injection pressure (marked 1 in Fig. 5). However, a significant breakthrough of gas occurred after the peak in injection pressure (marked 2 in Fig. 5), suggesting complex behaviour. The pressure then decreased towards steady state. The calculated NRVB

MODIFICATION IN CEMENT FLOW PROPERTIES

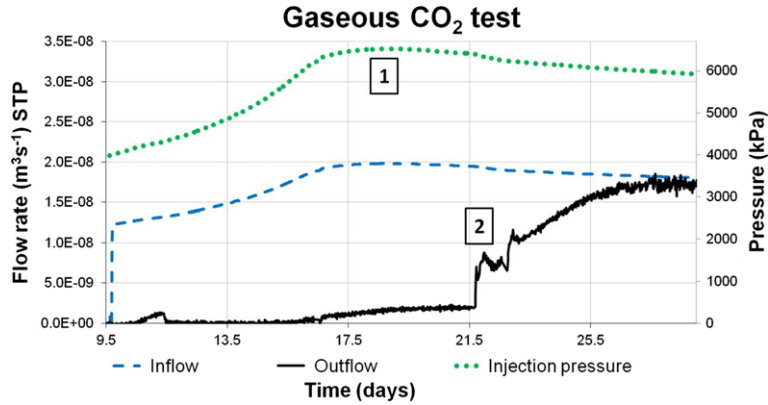


Fig. 5. CO₂ gas test showing the multiple breakthrough events lagging behind the main pressure peak during the experiment. Numbers within squares represent specific events during the experiment.

permeability halved in the presence of CO₂ gas compared to the N₂ base case, from 2.0×10^{-19} to 9.9×10^{-20} m². After gas testing had ceased, the pressure was allowed to decay naturally and the capillary was pressure determined. The capillary pressure was found to have doubled, relative to the N₂ gas test, from 300 to 600 kPa. The permeability of the carbonated cement to water was not tested in this instance.

Flow properties of supercritical CO₂
(Experiment 3)

A test using supercritical CO₂ was performed to assess the most extreme conditions under which cement carbonation may occur at 40 °C and 8 MPa. In this instance, a complex series of flow events were observed, resulting in four peaks in the

outflow flow rate (Fig. 6). The first peak (marked 1 in Fig. 6) is thought to relate to a small outflow of fluid displaced from the sintered distribution discs at the beginning of the gas injection. The remaining three peaks (marked 2, 3 and 4 in Fig. 6) were related to supercritical CO₂ in a series of breakthrough events that were initiated after the main pressure peak (marked 5 in Fig. 6). The resulting permeability (2.0×10^{-19} m²) was found to be the same as for the N₂ base case but was higher than with gaseous CO₂. Inspection of the NRVB core after testing showed that large areas of unreacted NRVB still remained. The area in which the CO₂ flowed was smaller overall than previous gas tests. The area over which permeability was calculated was, therefore, overestimated, resulting in a lower than expected permeability (in fact, lower than in the CO₂ gas test: see Table 2). We are unsure why a more direct pathway developed. Possibilities

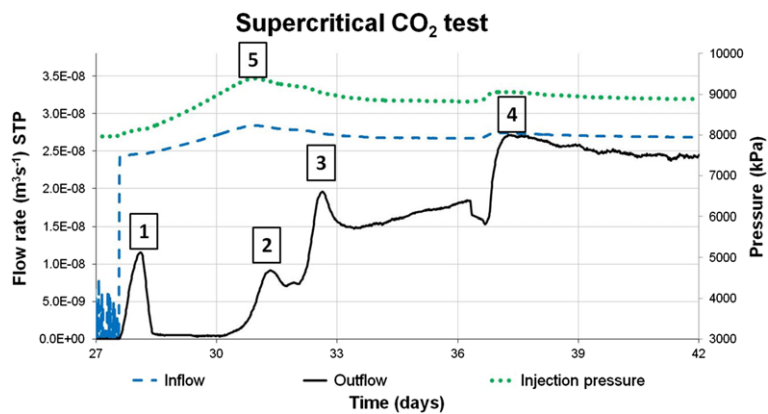


Fig. 6. Supercritical CO₂ test showing the complex breakthrough fronts of the fluid. Numbers within squares represent specific events during the experiment.

include that it could be related to the density of supercritical CO₂ or a fast pathway attributed to a potential heterogeneity in the sample. Further work is needed to identify which of these may have been operating.

Gas testing: investigation of the reaction zone (Experiment 4)

A gas test was conducted at 40 °C and 4 MPa using a single pump volume (500 ml) of gaseous CO₂ to allow the interface between unreacted and carbonated NRVB (i.e. the reaction zone) to be studied. The sample did not reach steady state in this instance, and the experiment was terminated after approximately half of the NRVB sample had been carbonated. After reaction, the NRVB core was cut in half and micropermeametry measurements were taken used to assess the small-scale variation in permeability across the reaction zone (Fig. 7). The recorded permeabilities were taken after the core had been subjected to vacuum desiccation, so are significantly higher than those produced in the gas test stages. However, micropermeametry provided an indication of the *relative* permeability change across the sample in relation to the main visible reaction zone. Permeability reduction was found to be greatest near the leading edge of the visible alteration front. This restriction is likely to account for the increased pressures observed during the CO₂ gas tests in comparison with the N₂ test.

Mineralogy

In the following subsections, we compare changes in the cement relative to its starting composition. Initially the cement was pale grey in colour, and comprised mainly fine-grained amorphous CSH (calcium silicate hydrate) material and portlandite.

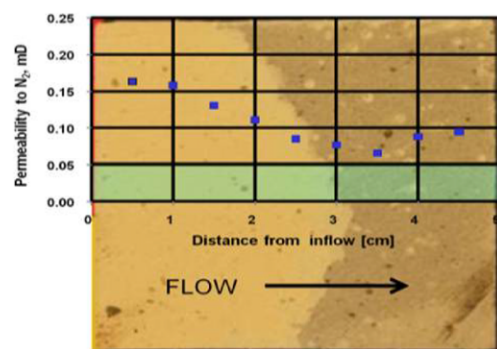


Fig. 7. Changes in micropermeability across the reaction zone of a sectioned core of partially carbonated NRVB cement, where 0.1 mD = $9.87 \times 10^{-7} \text{ m}^2$.

The cement also contained calcite from the limestone flour and traces of brownmillerite from clinker phases. The changes in the NRVB cement described in the subsequent subsections relate to Experiment 4 in which a core was partially carbonated, as this shows the most interesting mineralogical features relating to the reaction zones and reaction fronts.

Carbonation of NRVB

The fully carbonated core of NRVB after the gaseous CO₂ experiment (Experiment 2 in Table 1) showed clear changes in mineralogy in comparison to the unreacted core. There had been an almost complete replacement of the CSH and portlandite by calcium carbonate, mainly calcite and trace aragonite. Small voids present in the cement, created by air bubbles entrained during manufacture, had been lined and filled with secondary carbonates, tentatively identified as aragonite. The alteration of the sample was also apparent from the colour change of the NRVB. The fully carbonated sample had turned from grey to light brown in colour. This colour change was found to be associated with the release of ferric iron hydroxides from brownmillerite upon carbonation. Backscatter scanning electron microscopy-energy dispersive x-ray microanalysis (BSEM-EDXA) (Fig. 8) showed that the carbonated NRVB comprised a 'chicken-wire' meshwork of calcite-mineralized microfractures within a nanoporous matrix of amorphous silica and fine-grained patchy replacive calcite.

To determine the amount of CO₂ taken up by the cement, the completely carbonated sample of NRVB from Experiment 2 and an unreacted core were dried under vacuum. The unreacted core was

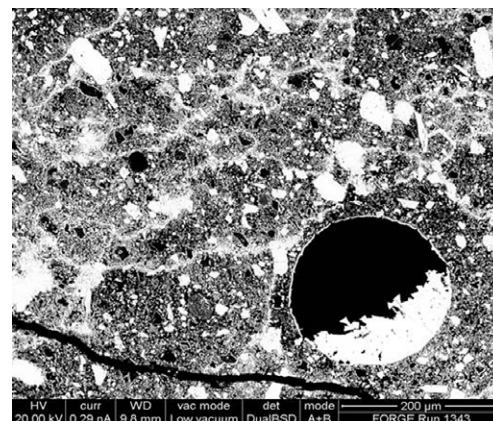


Fig. 8. An BSEM-EDXA image of densely calcite mineralized 'microfractures' giving a 'chicken-wire' appearance to the fully carbonated NRVB cement.

MODIFICATION IN CEMENT FLOW PROPERTIES

used to determine the initial saturation of the cement material and was found to contain approximately 30% extractable water; the carbonated sample contained only 20% extractable water, potentially reflecting mineralogical changes (a reduction in CSH) and also porosity changes due to carbonation. To determine the amount of carbonation, a portion of the unreacted or carbonated core was weighed accurately and then reacted with a known weight of 4 M HCl. The CO₂ uptake of NRVB was calculated to be 65 g of CO₂ for every 100 g of dry NRVB, a maximum 41% increase in dry weight.

Reaction front propagation mechanism

Carbonation produced a broad alteration zone, within which were a series of discrete, narrow reaction fronts (Fig. 9). These fronts moved through the sample at a rate governed by the ingress of CO₂. The reaction fronts advanced as small and short, but numerous, ‘protuberances’ that penetrated into the cement. These merged with adjacent features to make up what appeared to look like a single reaction

front at larger scales. In some instances, the reaction fronts enclosed and isolated pockets of partially altered cement behind them. The carbonated cement closest to the main reaction front comprised high-density carbonate precipitate, at the leading edge of which was a fine meshwork of what appeared to be calcite-filled ‘microfractures’. EDXA maps showed that there was enhanced calcium (Ca) concentration at the leading edge of this front (Fig. 10). Ahead of the carbonation front was an area of enhanced microporosity (Fig. 9). This area was depleted in Ca, associated with the dissolution of CSH phases and portlandite. The Ca from this area had migrated against the flow of CO₂ towards the carbonation front where it precipitated. Residual cement clinker grains were also found to be dissolved in this region, leaving small mouldic cavities partially lined with silica-rich material. The relatively uncarbonated cement (ahead of the main reaction front and labelled 3 in Fig. 9) contained some diffuse and patchy secondary carbonate but, on the whole, a significant amount of the CSH phases and Ca(OH)₂ were still intact.

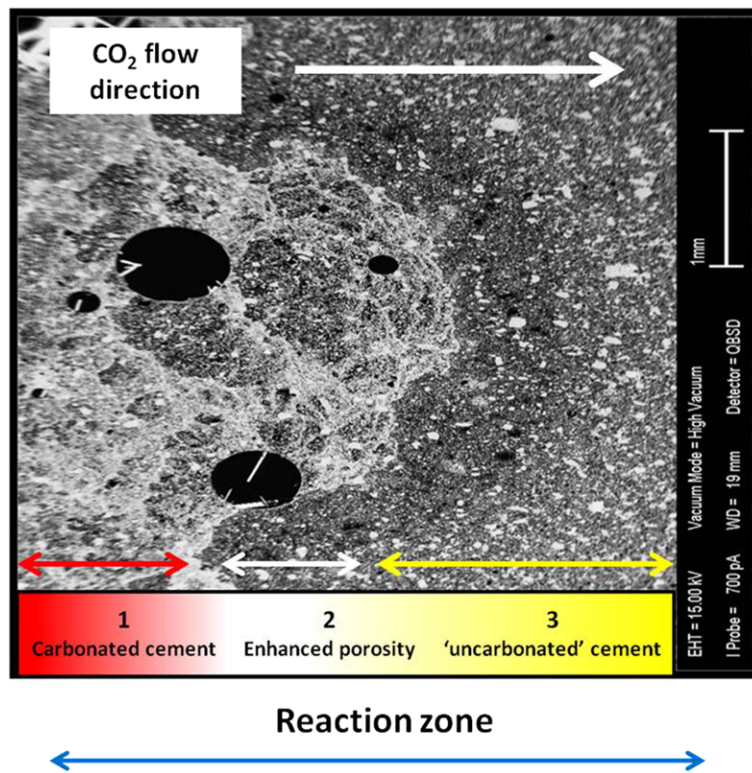


Fig. 9. SEM image showing distinct reaction fronts separating three areas making up the reaction zone: (1) the carbonated cement area, with fine ‘chicken-wire’ texture; (2) a zone of enhanced porosity from the dissolution reaction of the cement minerals; (3) the relatively intact and uncarbonated NRVB cement towards which the CO₂ is migrating.

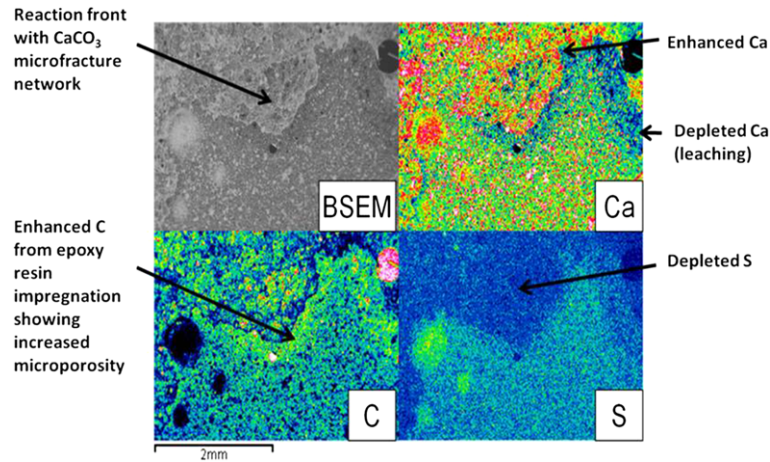


Fig. 10. A BSEM photomicrograph of the reaction zone together with element maps for calcium, carbon and sulphur showing the accumulation or depletion of each element.

1D modelling reaction-transport modelling

Predictive modelling was undertaken to help explain processes during carbonation rather than be an exact simulation of the experiments. PRECIP (Noy 1998), a single fluid-phase 1D reaction-transport code, was

used to simulate reactions occurring within the experiments. The experiment that was simulated was the dissolved CO_2 case. The initial sample was represented by a mix of tobermorite, calcite and portlandite, with a porosity of 52%. The initial pore fluid chemistry was chosen to be in equilibrium

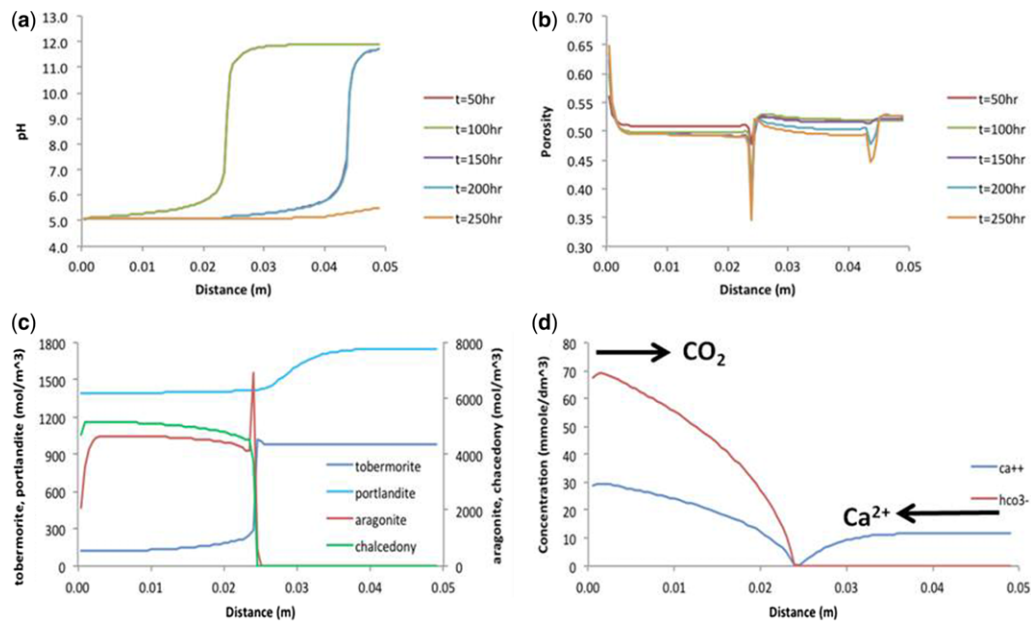


Fig. 11. 1D modelling of the ‘base case’ using PRECIP. (a) Change in pH over the 49 mm-long sample with the ingress of CO_2 over time. (b) Porosity changes occurring at distinct points over time as the reaction front moves along the length of the sample. (c) Concentrations of the starting and precipitated cement minerals across the length of the sample at 100 h after CO_2 injection. This was based on the reduced dissolution rate case. (d) Concentration of the species involved in aragonite precipitation at 100 h after CO_2 injection based on the reduced dissolution rate case.

MODIFICATION IN CEMENT FLOW PROPERTIES

with the mineral assemblage, with a calculated pH of 12.4. In the simulation, water was equilibrated with calcite and saturated with CO₂ at 4 MPa, and had a pH of 5. This aqueous fluid was then input into one face of the cement at a rate of 2000 μl h⁻¹ for the 49 mm-diameter modelled sample (double that of the experimental flow rate due to model run-time limitations). The simulation for the model resulted in a reaction zone, approximately 20 mm long, moving in a stepwise manner along the length of the sample. This zone, rather than a single reaction front, mirrors mineralogical observations of the carbonated cement from the experiments. The model predicted the initial transformation of tobermorite to aragonite and chalcedony, with a slower conversion of aragonite to calcite over time. Ingress of CO₂-saturated water reduced pH in the cement, producing a stepped pH profile along the core that was predicted to move through the core over time (Fig. 11). Predicted mineral changes were associated with the pH decreases. Spikes in aragonite precipitation were predicted over narrow regions. A small net reduction in overall porosity was predicted across the sample but the largest reductions in porosity occurred in the same narrow regions where aragonite precipitate formed. Predicted aqueous calcium concentrations drop to zero once the majority of the tobermorite had dissolved. Ca²⁺ then increased as portlandite began to dissolve. This decrease in Ca²⁺ was also observed in the experimental sample, producing a Ca-leached zone. The model predicted the back-diffusion of calcium ions against the pore water flow, resulting in a spike in aragonite precipitation through the complex interplay of differing rates of dissolution, precipitation, fluid flow and diffusion. The sharp 'peaks' in carbonate precipitation predicted by this 1D modelling work may offer an additional explanation to the apparently carbonate-filled 'microfractures'/'chicken-wire texture' described in the subsection on 'Carbonation of NRVB', as in two dimensions these 'peaks' could form narrow bands. Other simulations of the model were run with a faster tobermorite dissolution rate that produced more closely spaced aragonite precipitation points reflecting the importance of kinetics in these calculations (Purser *et al.* 2014). Further work is needed to ascertain whether these features are formed from a two-stage microfracturing–sealing process, or from a one-stage precipitation process.

Implications for a radioactive waste repository

Carbonation of NRVB cement resulted in the formation of reaction fronts that travelled through the samples. Portlandite and CSH phases were

destroyed, and amorphous silica and carbonate minerals were formed. This process is associated with localized porosity increases initially, which were subsequently variably filled with secondary CaCO₃. A zone of reduced permeability was created as the reaction front moved through the sample. This had the ability to 'armour' some regions of the cement, leading to isolated 'islands' of unreacted NRVB. This process could lead to a reduction in the predicted total buffering capacity of a given volume of cement. Overall bulk gas permeability was halved as a consequence of carbonation by gaseous CO₂. Carbonation resulting from the reaction of CO₂-saturated water was more significant, resulting in a three orders of magnitude reduction in permeability. Although reduced permeabilities in our tests resulted in increased pressures, in both cases it was still possible for gas to transmit along the length of the core of NRVB. These tests, however, were performed at an arbitrary flow rate of 1250 μl h⁻¹ and the CO₂ generation rates in a repository setting are currently undefined. Natural analogue studies (Rochelle & Milodowski 2013) of natural CSH phases that have been reacted with bicarbonate groundwaters at slower flow rates and millennia timescales show similar reaction mechanisms and mineralogical features as this experimental system. However, the far slower rates of carbonation in these natural systems appear to have produced very-low-permeability carbonate coatings that seal off the CSH from further reaction. This suggests that similar reactions occur over a wide range of timescales but that sealing may become more effective with increased time or with slower rates of reaction. However, further work is required in order to be able to upscale and understand the complex coupling between fluid flow, permeability and carbonation on a repository scale both in terms of duration and physical scale.

Conclusions

An experimental and modelling study has been conducted as part of the EC-funded FORGE project to investigate the impact of NRVB carbonation on flow properties. Carbonation of NRVB cement using CO₂ gas was found to halve the gas permeability of the cement in comparison with an inert gas such as nitrogen. The carbonation of NRVB by water containing dissolved carbon dioxide was found to have an even greater impact upon hydraulic permeability, reducing it by three orders of magnitude. Mineralogical assessment of the carbonated cement found significant reaction 'fronts' where the porosity had been redistributed, creating zones of increased porosity within extensively carbonated cement and immediately ahead of the main reaction

front, and decreased porosity at the leading edge of the main carbonation front. However, overall porosity was reduced as a consequence of carbonate precipitation. Of particular note is the precipitation of carbonate minerals in narrow bands throughout the carbonated area, resulting in a 'chicken-wire' texture. The presence of these narrow bands is thought to be key in controlling the overall reduction in the bulk permeability of the carbonated NRVB samples. The reduction in permeability upon carbonation could be advantageous with regard to sealing fractures and restricting the migration of radionuclides through groundwater percolation. However, the reduction in permeability could also inhibit the migration of gas from organic decomposition, leading to a build-up of pore pressure.

This work was supported through the European Atomic Energy Community, FORGE project, Grant Agreement No. 230357 and the Nuclear Decommissioning Authority Radioactive Waste Management Directorate (NDA/RWMD). This work is published with the permission of the Executive Director of the British Geological Survey, NERC.

References

- ATKINS, P. W. 1982. *Physical Chemistry*, 2nd edn. Oxford University Press, Oxford.
- CHAU, N., BAIRD, R. D. & ROGERS, V. C. 1995. Performance of reinforced concrete structures in low-level radioactive waste disposal units. In: AL-MANASEER, A. A. & ROY, D. M. (eds) *Concrete and Grout in Nuclear and Hazardous Waste Disposal*. American Concrete Institute, Detroit, Special Publications, **158**, 19–66.
- CROSSLAND, I. G. 1998. The role of engineered barriers in a UK repository for intermediate level radioactive waste. *Interdisciplinary Science Reviews*, **23**, 269–280.
- FABBRI, A., CORVISIER, J., SCHUBNEL, A., BRUNET, F., GOFFÉ, B., RIMMELE, G. & BARLET-GOUÉDARD, V. 2009. Effect of carbonation on the hydro-mechanical properties of Portland cements. *Cement and Concrete Research*, **39**, 1156–1163.
- FRANCIS, A. J., CATHER, R. & CROSSLAND, I. G. 1997. *Development of the Nirex Reference Vault Backfill; Report on Current Status in 1994*. Nirex Science Report S/97/014. Nirex Limited, Harwell, Oxfordshire.
- HARRINGTON, J. F. & HORSEMAN, S. T. 1999. Gas transport properties of clays and mudrocks. In: ALPIN, A. C., FLEET, A. J. & MACQUAKER, J. H. S. (eds) *Muds and Mudstones: Physical and Fluid Flow Properties*. Geological Society, London, Special Publications, **158**, 107–124.
- NOY, D. J. 1998. *User Guide to PRECIP, a Program for Coupled Groundwater Flow and Reactive Solute Transport*. British Geological Survey Technical report WE/98/13.
- PURSER, G., ROCHELLE, C. A., MILODOWSKI, A. E., NOY, D. J., HARRINGTON, J. F., WAGNER, D. & BUTCHER, A. S. 2014. *Modification to the Flow Properties of Repository Cement as a Result of Carbonation*. British Geological Survey Internal Report, OR/14/003. British Geological Survey, Keyworth, Nottingham.
- ROCHELLE, C. A. & MILODOWSKI, A. E. 2013. Carbonation of cement seals: comparing evidence from short-term laboratory experiments and long-term analogues. *Applied Geochemistry*, **30**, 161–177.